Controlling the Phase and Amplitude of Plasmon Sources at a Subwavelength Scale

G. Lerosey,[†,||] D. F. P. Pile,[†] P. Matheu,[†] G. Bartal,[†] and X. Zhang*,[†,‡]

NSF Nano-scale Science and Engineering Center, University of California, 5130 Etcheverry Hall, Berkeley, California 94720-1740, and Materials Sciences Division, Lawrence Berkeley National Laboratory, 1 Cyclotron Road, Berkeley, California 94720

ABSTRACT

We present a new class of nanoscale plasmonic sources based on subwavelength dielectric cavities embedded in a metal slab. Exploiting the strong dispersion near the Fabry−Perot resonance in such a resonator, we control the phase and the amplitude of the generated plasmons at the subwavelength scale. As an example, we present a subwavelength unidirectional plasmonic antenna utilizing interference between two plasmonic cavity sources with matched phase and amplitude.

Surface plasmons polaritons (SPPs) are collective excitations of electrons coupled to an electromagnetic field at the interface between a dielectric and a metal.[1] Their evanescent nature along the normal to the metal/dielectric interface allows subwavelength confinement that can be significantly smaller than diffraction limited optical waves in bulk media. SPPs, therefore, are ideal candidates for the construction of subwavelength optical devices. In the past few years, SPPs have also been identified to be the major physical mechanism involved in the extraordinary transmission of light (ETL) through metal films with subwavelength holes which was first reported by Ebbesen et al.[2,4] Subsequent studies have been made on uniform periodic arrays of holes, slits, and more complex shapes fabricated in metallic films. Those studies demonstrate that one can take advantage of the interference between plasmons generated on metal films by uniform periodic sources (e.g., slits or holes in metal films) to, for instance, focus or disperse light,[5,6] or realize ETL.[7] Naturally, for flexible control and manipulation of light by such metal films it is necessary to evolve beyond the uniform periodic sources in refs 2−7 and introduce the rich possibilities afforded by nonuniform source films.

When light enters a subwavelength dielectric structure in a metallic film, a significant fraction, if not all, of the light propagates through the film as surface plasmons that are confined at the metal/dielectric interfaces. For example, transverse magnetic (TM) polarized light impinging on a silver film containing air gaps gives rise to waves known as gap plasmons (GPs), whose properties are closely related to the dimensions of the gaps: the smaller the gap width, the larger the wavenumber of the GP.[11,12] This way, one can design sources of plasmons with arbitrary phase by adjusting the width of the gap. Similarly, one can fill the air gaps with different dielectrics hence inducing an optical path length between the generated plasmons.[8,10] Those two approaches are quite inflexible and practically hard to fabricate.

In order to realize surface plasmon sources with chosen phase and amplitude, our approach utilizes the gap plasmon dispersion relation along with Fabry−Perot (FP) resonances in a cavity.[13,14] Air gaps in metal films typically display low-efficiency FP resonance[13] that, as we explain later, can be increased by introducing highly reflective "mirrors" on both sides of the metal film. Sharper resonance results in longer propagation of the GPs in the gaps due to constructive interference and multiple reflections in the cavity. Hence, the relative phase accumulation at the output side for slits of varying widths is increased regardless of the metal film thickness. Our cavity design corresponds to a forced mechanical oscillator: when driven below, at, and above the resonance frequency, the response lags, matches, or leads in phase.[15] Namely, tuning the width of the gap, or equivalently the GP wavenumber, allows a control of the phase and amplitude of the generated SP.

* Corresponding author: xiang@berkeley.edu.
† NSF Nano-scale Science and Engineering Center, University of California.
‡ Materials Sciences Division, Lawrence Berkeley National Laboratory.
|| Currently at Laboratoire Ondes et Acoustique, École Supérieure de Physique et de Chimie Industrielles, Université Paris VII, Centre National de la Recherche Scientifique, UMR 7587, 10 rue Vauquelin, 75005 Paris, France. E-mail: geoffroy.lerosey@espci.fr.
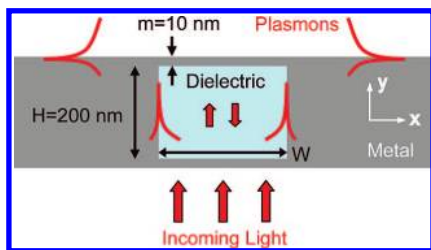
Figure 1. A schematic representation of the gap plasmon cavity.

To illustrate this new mechanism, we present a simple design consisting of only two parallel cavities of different widths. We show that such a system realizes a unidirectional plasmonic antenna similar to the one that was studied very recently by López-Tejeira et al.[16] In our unidirectional antenna, however, the lateral size can be reduced to half a plasmon wavelength (compared to a minimum size of several wavelengths in ref 16). Additionally, the top surface of our antenna is flat, which may prove useful for many applications such as sensing. Furthermore, using both the gap plasmon dispersion relation and the metal mirrors allows us to provide a design that does not use an unrealistically small slit width[9] or very difficult fabrication procedures such as filling different slits with different dielectrics.[10]

We start by studying one cavity by itself. The metal used is gold, and we work at the telecom wavelength of 1.53 μm. As mentioned above, a slit Fabry−Perot resonance is inefficient because of excessive radiation damping due to poor reflection from the terminated slits.[17] One solution to overcome this problem is to introduce highly reflective, semitransparent, thin metallic mirrors at each end of the slit. The thickness of the metallic mirrors influences two parameters. First, adding a metallic layer creates a change of impedance at the boundaries of the dielectric filled slit, which causes the gap plasmons to reflect on those boundaries. Hence the Q-factor increases, and the thicker the film, the larger the impedance mismatch and the larger the Q-factor of the cavity. Second, the effective cavity length varies due to the finite permittivity of the metal. We have performed various simulations (not presented here) in order to evaluate quantitatively the effect of the metallic mirrors. The Q factor, which is about 5 for a slit filled with Ta_2O_5 as in our design, rises to 10 for 10 nm wide gold mirrors and increases again for wider films, until it saturates around 22 for 30 nm films due to propagation losses inside the cavity. The resonant wavelength is also affected by the width of the semitransparent mirrors. Indeed, without mirrors it is about 1250 nm since the slit is terminated by low permittivity dielectric (air). Introducing the mirrors shifts this wavelength to 1530 nm for 10 nm wide films due to penetration of the field in the metal, and then for wider films it slowly decreases again toward 1420 nm. In the following demonstration, we will focus on gold-film mirrors approximately 10 nm thick which provide, as we explain later, SPPs with amplitude and phases that fit our antenna design. For practical purposes, one mirror is placed on a supporting substrate while the second, or upper, mirror lies on top of a dielectric filler material.
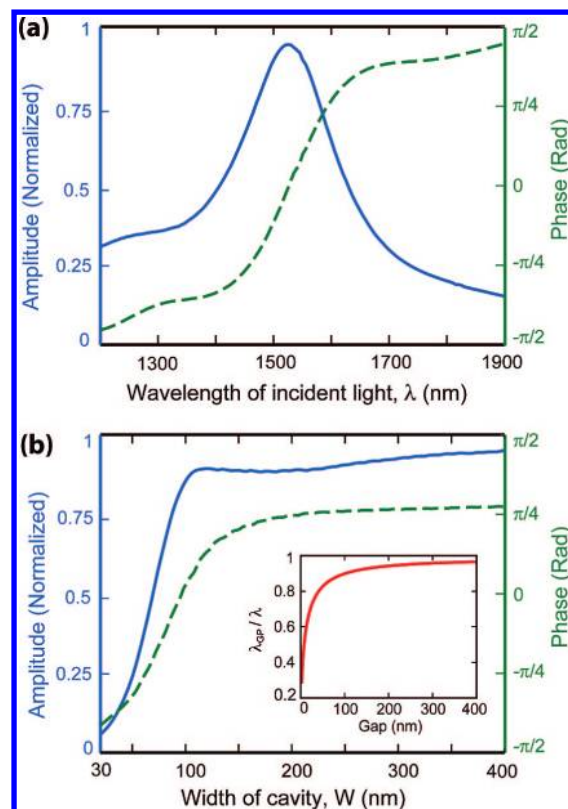
Figure 2. (a) Dependence of source amplitude (solid curve and left axis) and phase (dashed curve and right axis) on vacuum wavelength of the incident light. Gap width is kept constant, W_R = 100 nm which has the designed resonant wavelength of 1530 nm. (b) Dependence of source amplitude (solid curve and left axis) and phase (dashed curve and right axis) on gap width, W_R, for a constant wavelength of 1530 nm. The inset represents the dependence of the gap plasmon wavelength as a function of the gap width.

A single cavity structure, detailed in the Figure 1, is numerically investigated using a finite-element frequency-domain method (Comsol Multiphysics) for the solution of the Maxwell's equations. The complex frequency-dependent gold permittivity is set to $\varepsilon_m = -127 + 11i$,[18] while the refractive index of the dielectric is set to $n_d = 2.3$ corresponding to Ta_2O_5. The cavity structure lies on a quartz substrate with a refractive index $n_s = 1.5$, and the cavity is illuminated by a TM polarized plane wave through the substrate (electric field parallel to the x axis). We consider infinite slits along the z axis (Figure 1) reducing the numerical simulation to a simple two-dimensional problem.

Figure 2a (solid line) shows the amplitude of the plasmons at the output of the cavity, that is to say of the plasmons generated on the upper interface of the slab and propagating along the x axis, as a function of the incident wavelength. We use the aforementioned parameters as well as the following dimensions: a slit with width $W_R = 100$ nm, a gold metal film thickness $H = 200$ nm, and thin gold mirrors with thicknesses $m = 10$ nm. The resonant wavelength of this structure is $\lambda_0 = 1530$ nm with a calculated Q-factor of 10, defined as the central wavelength divided by the bandwidth at half intensity. Figure 2a also displays the phase (dashed line) of the output plasmons at the top metal surface.

The cavity structure design is again verified by noting that the extracted phase ranges from approximately $-\pi/2$ to $\pi/2$ for wavelengths between 1200 and 1900 nm with zero phase difference at 1530 nm. We calculate the phase and amplitude of the plasmons at the output of the cavity using the magnetic component of the plasmonic field at a distance of 1 plasmonic wavelength of the edges of the cavity in the x direction and at the metal/dielectric interface. This is achieved using a mode-matching technique as described in ref 19, where the magnetic field at a certain abscissa is projected on the plasmonic mode and integrated, hence giving access to a coefficient that contains both the phase and amplitude of the plasmonic field at the x position.

Recalling the goal of obtaining sources of plasmons at a given wavelength λ_0 with a desired phase and amplitude, we study the effects of changing the width of the slit on the phase (dashed line) and the amplitude (solid line) of the waves exiting the cavity, presented in Figure 2b. As expected, the output phase (at a constant frequency) follows the same trend when W ranges from 30 to 100 nm, starting around $-\pi/2$ and crossing zero at $W_R = 100$ nm as designed. On the other hand, it varies over a smaller range from 100 to 400 nm and saturates near $\pi/4$. The behavior of the plasmon wave amplitude follows the same trend. Indeed, this parameter is maximized for the resonant width of the slit but does not tend to zero when the width of the cavity is increased beyond its resonant value. In fact the output plamons amplitude decreases first due to cavity detuning and then slowly increases again from $W = 200$ to 400 nm because of a slightly more efficient coupling of the incoming light to gap plasmons that is due to a geometric effect.

The behaviors of the extracted phase and amplitude from the previous simulations can be explained qualitatively by a simple model of a conventional Fabry−Perot cavity. One can express the phase of the output waves of a Fabry−Perot cavity as a function of the Q-factor (Q), the resonant wavelength (λ_0), and the wavelength of the waves (λ)

$$\phi \approx \operatorname{atan}\left(Q\frac{(\lambda - \lambda_0)}{\lambda_0}\right) \quad (1)$$

Similarly, given the input amplitude A_0, the output amplitude A writes

$$A \approx A_0 \frac{\lambda_0}{\sqrt{\lambda_0{}^2 + Q(\lambda_0 - \lambda)^2}} \quad (2)$$

Thus, when we study cavities with a fixed width (or equivalently for a fixed λ_0), the phase and amplitude of the plasmons at the output of the cavity depend on the Q-factor of the cavity as follows: a higher Q-factor increases the phase range for output plasmons but narrows the output amplitude peak and decreases the output plasmon generation efficiency out of the resonance. Then, when the incident wavelength varies below and above the resonant wavelength of the cavity, the amplitude shows a typical even dependency and reaches its maximum at the λ_0, while the phase starts from a negative value limited by the Q-factor, crosses 0 at λ_0, and increases again.

Similarly, the analysis for a varying cavity width (or equivalently a varying λ_0) is fairly straightforward. When
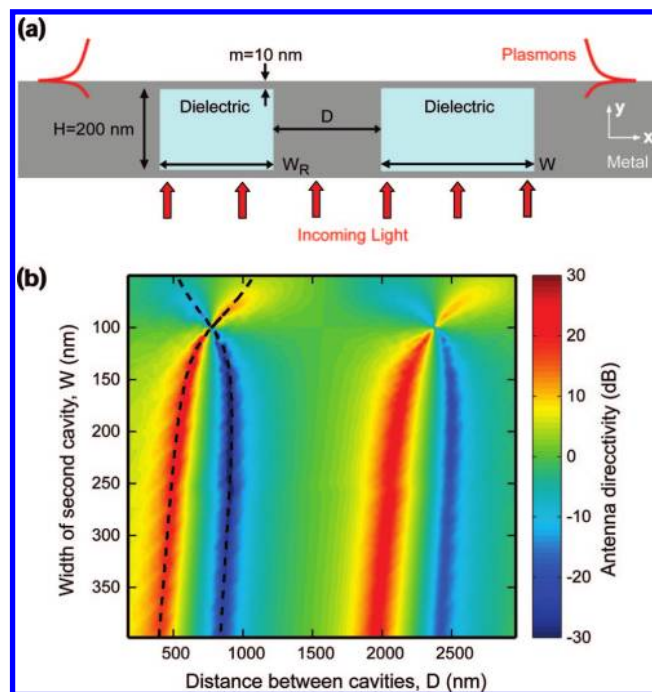

Figure 3. (a) A schematic representation of the plasmonic antenna consisting of a pair of gap plasmon cavities. (b) Directivity in decibel of the plasmonic antenna (indicated by the color scale) for varying width of the second cavity, W, and distance between the two cavities, D. The dashed curve is a parametric plot of eq 5 for $n = 0$.

the width is smaller than W_R for $\lambda_0 = 1530$ nm, the GP wavelength (λ_{GP}) depends strongly on the gap width, as can be see by the steep portion of the GP dispersion relation (inset of Figure 2b). In this steep region, the phase swings quickly from a minimum value (limited by the Q-factor) to zero and the amplitude follows the same trend as the phase. On the contrary, while the width is increased above the resonance, λ_{GP} does not vary significantly, in the flatter portion of the dispersion relation. In other words, for very wide gaps, λ_{GP} remains close to 1530 nm, the phase saturates around $\pi/4$, and the output plasmon amplitude stabilizes. Once again, if the Q-factor is increased (e.g., by using thicker mirrors) the phase can vary over a broader range (between $-\pi/2$ and $\pi/2$), and the output amplitude is decreased accordingly since a small variation in width leads to complete detuning of the cavity due to off-resonance conditions. Conversely, one can set the resonant width of the cavity to a lower value, in the abrupt part of the GP dispersion relation, in order to get the same effect.

Essentially, our numerical simulations and our qualitative explanation show that we can design sources of plasmons with different relative phases and amplitudes. Our unidirectional plasmonic antenna design calls for sources of plasmons with equal amplitudes, and hence, the associated phase shift is relatively limited by a low Q-factor for the small values of W and the GP dispersion relation for the higher values of W.

A unidirectional antenna, depicted in Figure 3a, uses two GP cavities as described in detail below. The first cavity, resonant at λ_0 with $W_R = 100$ nm, generates plasmons with
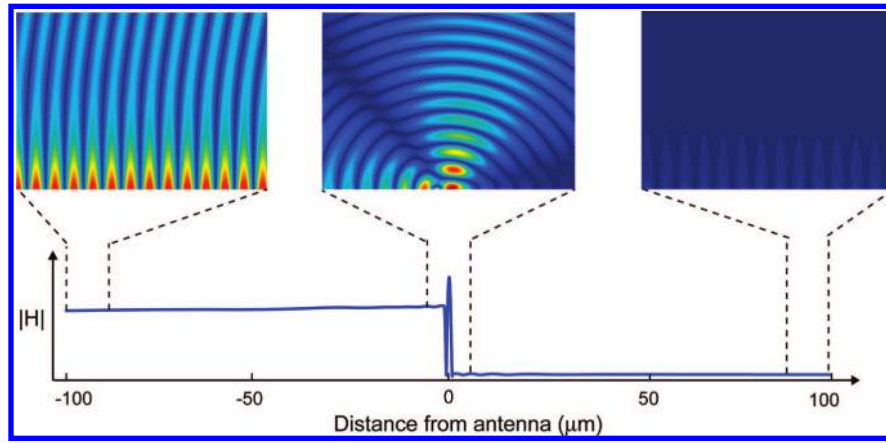
Figure 4. Dependence of the time average of the magnetic field, H, on distance from the antenna (bottom plot). Instantaneous magnetic field amplitude in the x-y plane near the antenna (top middle), and far from the source (top left and top right). The field on the top middle map has been divided by 10 to fit the same color map. The origin of the x axis is between the two cavities.

zero phase. A second cavity, placed a distance D from the first cavity, has a width W and generates plasmons with a relative phase difference ϕ. All other parameters remain the same. For fabricated cavities at least a few wavelengths deep along the z axis, we can reduce the analytical problem to one dimension (x axis). For this reason the field strength of the cavity-generated surface plasmons remains approximately constant along the direction of propagation (along the axis). This assumption is valid for weak dissipation or large propagation distances compared to the cavity separation D. Assuming equal amplitude sources, the plasmon field created by the antenna can be written as the sum of the two Green's functions[20]

$$s_1 = e^{i(k_{sp}|x-D/2|)} \quad \text{and} \quad s_2 = e^{i(k_{sp}|x+D/2|+\phi)} \qquad (3)$$

Here, k_{sp} is the surface plasmon wave vector and D is the distance between the two cavities. Then we can write the harmonic amplitude of the field on either side of the structure

$$F^L = (1 + e^{i(k_{sp}D-\phi)}) \quad \text{and} \quad F^R = (1 + e^{i(k_{sp}D+\phi)}) \qquad (4)$$

Equation 4 demonstrates the directionality of the antenna; to generate a surface plasmon propagating only in the positive (respectively negative) x direction, we set, with n any integer

$$k_{sp}D \pm \phi = \pi + 2n\pi \qquad (5)$$

Figure 3b shows a map of the antenna directivity, defined as the ratio between the intensities of the plasmonic field amplitudes on each side of the structure, as a function of both ϕ (or W) and D. The map indicates both positive and negative directionality as well as the strength of directionality for W between 50 and 400 nm and D between 100 nm and 3 μm. The directivity exactly follows the parametric curve given by eq 5, represented by the dashed black line for $n = 0$. Furthermore, varying the cavity width produces amplitude differences that are clearly visible in Figure 3b. In fact, the directivity is quite low for small values of W, consistent with the low efficiency for small slit widths described above (see Figure 2b). As expected, there is a maximum of directivity for $W = 200$ nm, and the degree of directivity can be traced by following the dashed curve plotted in Figure 3b. Finally, in Figure 4, we plot the instantaneous modulus of the total magnetic field created by the antenna, for a second slit width

of 300 nm, and a separation $D = 340$ nm, hence verifying eq 2. Clearly plasmons are generated only on the left side of the metal film.

We note here that the bulk waves are also sent in the same directions as the plasmons. This is due to the fact that at 1530 nm the wavenumber of the plasmons does not differ much from one of the waves in free space. This would be much different in the visible region, especially toward the low wavelengths, since the wevanumber of bulk waves would then be drastically different than that of SPs. We underline also that here we have chosen to use two cavities with similar amplitudes, hence limiting the phase difference between them through the Q-factor. It is possible to use cavities with really different amplitudes, by for example increasing the number of low efficiency cavities and spacing them correctly to allow the constructive interference of surface plasmons.

Finally, several avenues remain for future investigation. First, although our studies have been carried out with linear slit cavities for the sake of simplicity, our conclusions can be extended to any cavity shape—for example, circular rings as plasmon sources with arbitrary phase. Second, the cavities described in this paper can be used in many applications. A periodic structure with a unit cell consisting of two cavities with one presenting a phase lag holds scientific and engineering merit. Similarly, one can imagine a periodic assembly of such GP cavities presenting subperiodic patterns of phase and amplitude differences, hence creating a new kind of ETL. Third, nonperiodic and nonuniform arrays of such unit cells may result in customizable generation of subwavelength fields of arbitrary phase and amplitude everywhere on the film. Finally, while the source is in nature plasmonic in order for it to be subwavelength, the output field is not limited specifically to plasmons but any availabe eigenmodes of its environment like bulk waves for example. Experiments and fabrication are underway for the structures proposed in this paper. One approach uses focused ion beam milling to etch slits in a metal film and physical vapor evaporation to deposit both the dielectric material and thin film mirrors. Another fabrication approach under consideration uses electron beam lithography combined with a plating solution to grow a gold film around dielectric structures.

To conclude, we have presented a new class of nano-optical plasmonic sources based on subwavelength gap plasmon cavities designed with moderately narrow slits that are filled with a dielectric material and mirrored with a thin metallic film at each end. Such a structure allows control over the phase and amplitude of the plasmons excited in the cavity via the widths of the slits and the metallic mirrors. This structure provides a new platform for the design of surface plasmon based devices. Furthermore, it allows one to fabricate several different sources within the same metal film while the output side of the film remains planar. We have illustrated our approach by designing a unidirectional plasmonic antenna at the wavelength of 1530 nm using only two cavities. A periodic arrangement of cavities with carefully chosen dimensions for the desired phase broadens the spectrum of applications of ETL and related phenomena. We believe this concept can be extended to numerous optoelectronic parts based solely or partly on surface plasmons.

References

(1) Raether, H. *Surface Plasmons: On Smooth and Rough Surfaces and on Gratings*; Springer: Berlin, 1988.
(2) Ebbesen, T. W.; Lezec, H. J.; Gaemi, H. F.; Thio, T; Wolff, P. A. Extraordinary optical transmission through sub-wavelength hole arrays. *Nature* **1998**, *391*, 667.
(3) Popoff, E.; Neviere, M.; Enoch, S.; Reinisch, R. Theory of light transmission through subwavelength periodic hole arrays. *Phys. Rev. B.* **2000**, *62*, 16100.
(4) Martin-Moreno, L.; Garcia-Vidal, F. J.; Lezec, H. J.; Pellerin, K. M.; Thio, T.; Pendry, J. B.; Ebbesen, T. W. Theory of extraordinary optical transmission though subwavelength hole arrays. *Phys. Rev. Lett.* **2000**, *86*, 1114.
(5) Lezec, H.J.; Degiron, A.; Devaux, E.; Linke, R.A.; Martin-Moreno, L.; Garcia-Vidal, F. J.; Ebbesen, T. W. *Science* **2002**, *297*, 820.
(6) Mikhailov, V.; Wurtz, G. A.; Elliot, J.; Bayvel, P.; Zayats, A. V. Dispersing light with surface plasmon polaritonic crystals. *Phys. Rev. Lett.* **2007**, *99*, 83901.
(7) Garcia de Abajo, F. J. Colloquium: light scattering by particle and hole arrays. *Rev. Mod. Phys.* **2007**, *79*, 1267.
(8) Shi, H; Lu, X.; Du, C. Young's interference of double nanoslit with different widths. *Opt. Express* **2007**, *15*, 11321.
(9) Shi, H.; Wang, C.; Du, C.; Luo, X.; Dong, X.; Gao, H. beam manipulation by metallic nanoslits with variant widths. *Opt. Express* **2005**, *13*, 6815.
(10) Xu, T.; Zhao, Y.; Gan, D.; Wang, C.; Du, C.; Luo, X. Directional excitation of surface plasmons with subwavelength slits. *Appl. Phys. Lett.* **2008**, *92*, 101501.
(11) Dionne, J. A.; Sweatlock, S. A.; Atwater, H. A.; Polman, A. Plasmon slots waveguide: towards chip-scale propagation with subwavelength-scale localization. *Phys. Rev. B* **2006**, *73*, 35407.
(12) Pile, D. F. P.; Ogawa, T.; Gramotnev, D. K.; Matsuzaki, Y. Two-dimensional localized modes of a nanoscale gap plasmon waveguide. *Appl. Phys. Lett.* **2005**, *87*, 261114.
(13) Takakura, Y. Optical resonance in a narrow slit in a thick metallic screen. *Phys. Rev. Lett.* **2000**, *86*, 31.
(14) Miyazaki, H. T.; Kurokawa, Y. Squeezing visible light waves into a 3-nm-thick and 55-nm-long plasmon cavity. *Phys. Rev. Lett.* **2006**, *96*, 097401.
(15) Landau, L. D.; Lifshitz, E. M. *Mechanics*, 3rd ed.; Course of Theoretical Physics; Butterworth-Heinemann: Oxford, 1993; Vol. 1, Chapter 5.
(16) Lopez-Tejeira, F.; Rodrigo, S. G.; Martin-Morino, L.; Garcia-Vidal, F. J.; Devaux, E.; Ebbesen, T. W.; Krenn, J. R.; Radko, I. P.; Bozhevolnyi, S. I.; Gonzales, M. U.; Weeber, J. C.; Dereux, A. Efficient unidirectional nanoslit couplers for surface plasmons. *Nat. Phys.* **2007**, *3*, 324.
(17) Pacifici, D.; Lezec, H.; Atwater, H.; Weiner, X. Quantitative determination of optical transmission through subwavelength slit arrays in Ag films: Role of surface wave interference and local coupling between adjacent slits. *Phys. Rev. B* **2008**, *77*, 115411.
(18) Johnson, P. B.; Christy, R. W. Optical constants of the nobel metals. *Phys. Rev. B* **1972**, *6*, 4370.
(19) Oulton, R. F.; Pile, D. F. P.; Liu, Y.; Zhang, X. Scattering of surface plasmon polaritons at abrupt surface interfaces: implications for nanoscale cavities. *Phys. Rev. B* **2007**, *76*, 35408.
(20) These quantities assume an incoming plane wave that is directed perpendicularly to the slab of metal. If the plane wave has an angle with the normal of the metal slab, one should take into account the difference of optical path length induced by such an angle between the two cavities. More generally, the shape of the incoming light beam should be taken into account when designing and optical device using such plasmonic sources.

NL803079S